HOKKAIDO UNIVERSITY

Title	Homogeneous Large-Scale Synthesis of GaAs/GaInNAs/GaAs Nanowires on a Si Wafer for Devices Operating in the Near-Infrared Region
Author(s)	Minehisa, Keisuke; Nakama, Kaito; Hashimoto, Hidetoshi et al.
Citation	ACS Applied Nano Materials, 7(18), 21852-21859 https://doi.org/10.1021/acsanm.4c03855
Issue Date	2024-09-13
Doc URL	https://hdl.handle.net/2115/95964
Rights	This document is the Accepted Manuscript version of a Published Work that appeared in final form in ACS Applied Nano Materials, copyright © American Chemical Society after peer review and technical editing by the publisher. To access the final edited and published work see http://pubs.acs.org/articlesonrequest/AOR-PKCS8TKD2ZVUCU9YHU7B.
Type	journal article
File Information	Minehisa_Primary Manuscript2-2.pdf

Hokkaido University Collection of Scholarly and Academic Papers : HUSCAP

Homogeneous Large-Scale Synthesis of GaAs/GaInNAs/GaAs Nanowires on a Si Wafer for Devices Operating in the Near-Infrared Region

Keisuke Minehisa, Kaito Nakama, Hidetoshi Hashimoto, Fumitaro Ishikawa**

Research Center for Integrated Quantum Electronics, Hokkaido University, North 13 West 8, Sapporo, 060-0813, Japan

*Corresponding authors
E-mail: minehisa.keisuke@rciqe.hokudai.ac.jp (K. M.),
ishikawa.fumitaro@rciqe.hokudai.ac.jp (F. I.)

ABSTRACT

The synthesis of semiconductor nanowires (NWs) with near-infrared light-absorbing and emission properties is presented. Gallium (Ga)-induced vapor–liquid–solid growth is used to produce GaAs/GaInNAs/GaAs core–multishell NWs on a 2-inch Si(111) wafer using plasma-assisted molecular beam epitaxy. The GaInNAs shell consists of 11% indium (In) and varying compositions of nitrogen (N) up to 1.9%. The NWs serve as an anti-reflective material, showing that the entire substrate is black. Photoluminescence measurements at room temperature validate the expansion of the operating wavelength into the near-infrared region as the N content in the NWs increases. The GaInNAs sample with 11% In and 1.2% N shows homogeneous luminescence at 1100 nm across the entire 2-inch Si substrate. The reflectance of the NW samples is low, less than 2%, and the absorption edge can be controlled by modifying the composition of In and N indicating the potential application of large-scale photoelectric conversion such as solar cells.

KEYWORDS: nanowires, molecular beam epitaxy, III-V compound semiconductors, silicon, luminescence, reflectance

1. INTRODUCTION

Nanowires (NWs) are one-dimensional semiconductor materials that are characterized by their thin structure and valued for their configuration and potential applications in opto-electronic devices, such as light-emitting devices, laser diodes, solar cells, and high-electron mobility transistors.[1-9] Gallium arsenide (GaAs), classified as a III–V compound semiconductor, is known for its superior electron mobility and high photoelectric conversion efficiency. The epitaxial process of growing III–V semiconductors on Si platforms is difficult because of the large variation in thermal expansion coefficients and lattice constants between the two materials. The advanced epitaxial techniques enable the heteroepitaxial growth of III–V semiconductor NWs on silicon (Si) wafers.[10, 11] After the formation of the NW core, the conditions can be modified to promote radial growth. This heterostructure can improve the performance of devices.[12-18] In particular, NWs-based solar cells with core–shell heterostructures can significantly enhance the performance due to the light absorption along the NWs' long axis and the efficient radial separation and collection of photo-generated carriers.[19, 20] Additionally, intermediate-band solar cells (IBSCs) incorporating dilute nitride III-N-V compounds within III-V NW heterostructures are also expected to lead to a novel photovoltaic cell with unprecedentedly high power conversion efficiency, simpler junction geometries, reduced structural constraints, lower material usage and thus associated fabrication costs.[21] III-N-V based core–multishell NWs for radial junction IBSCs proposed by P. Prete et al., promise to overcome the limitations of planar IBSCs using dilute nitride III-N-V compounds, i.e. the reduced carrier diffusion lengths and the relatively low absorptance.[21] Emphasizing large-scale production and macroscale applications is necessary to achieve high-efficiency energy conversion devices using NW, as well as significant outputs.[22, 23] Metalorganic vapor-phase epitaxy, molecular beam epitaxy (MBE), and chemical-beam epitaxy are common techniques that are used for producing III–V NWs with desirable properties.[22] Nonetheless, the report of achieving a large volume of III–V NWs on Si is limited because of the high cost of growth capacity.[22]

Recently, we have utilized MBE to produce high-quality GaAs/AlGaAs core–shell NWs on a entire 2-inch Si substrate, which was achieved through Ga-induced vapor–liquid–solid growth.[24] This growth procedure was performed without the use of pre-treatments such as film deposition or patterning. Remarkably, after the formation of NWs, the entire substrate has a black color and a low reflectance at the GaAs absorption edge, indicating that the semiconductor material serves as a highly anti-reflective material. K. Amemiya et al. reported “supreme black” materials with exceptionally low reflectance of less than 0.0002, which was

attributed to a microcavity surface texture with nanoscale features.[25] This result demonstrates a nearly perfect anti-reflective performance; nevertheless, it does not function as a semiconductor. We then developed a mechanism to produce light-absorbing materials with the black properties using GaAs-related heterostructure NWs of high quality, high density, and homogeneity.[24] Notably, due to their small diameter (subwavelength), NWs have a large absorption cross-section associated with the nano-antenna effect. Indeed, P. Krogstrup et al. calculated the absorption cross-section near the fundamental band gap to be 1×10^6 nm^2 for a GaAs NW diameter of 380 nm.[26] This allows the NW density required to efficiently absorb solar photons incident on a NW array to be reduced to the range of 10^8 cm^{-2}, which is very similar to the NW density of our fabricated samples.[21] Additionally, it has been reported that in GaAs/AlGaAs NWs with a core–shell structure, light wave-guiding of incident light into the GaAs core can be improved by properly engineering the shell material's thickness, leading to enhanced optical absorption compared to unpassivated NWs.[27] Furthermore, dense arrays that involve antireflection, nano-antenna, and light-guided mode effects not only enable high optical absorption of solar radiation but also require only 10-20% of the total NW volume needed for planar epilayers of the same thickness as the NW average height. This significantly reduces the volume of costly III-V compounds used. Dilute nitride GaInNAs alloys, a few % of nitrogen is introduced into the host GaInAs matrix, allow engineering of the band gap, band structure, and lattice constant through modifications to the In and N compositions. These features make them attractive for applications in infrared light emitters and advanced solar cell structures operating in the near-infrared (NIR) region.[28-35]

In our previous report,[35] we used a patterned Si substrate with a precisely controlled SiO_2 mask. In that report, we demonstrated that by expanding the available range of As pressure during growth to reduce crystal defects, we could achieve the growth of well-defined and position-controlled NWs with high-quality light-emitting properties. In contrast, in this report, we use epi-ready Si substrates without any pretreatment to achieve cost-effective growth suitable for the large volume synthesis of NWs.[24] Here, we synthesized a large quantity of randomly positioned NWs across the entire substrate and demonstrated their characteristic high absorption properties from visible-to-NIR wavelengths. We also show that good light-emitting performance from quantum-well structures can be maintained under appropriate conditions. These findings suggest future prospects for the integration of light-absorbing and light-emitting devices, such as solar cells and lasers, on the substrate. In this paper, we present the growth of high-quality and homogeneous GaAs/GaInNAs/GaAs core–multishell NWs with room temperature photoluminescence (RT-PL) at emission wavelengths exceeding 1 μm

across the 2-inch Si wafer, and their absorption edges are controlled by adjusting the composition of In and N exhibiting high absorption and black features.

2. EXPERIMENTAL DETAILS

2.1. Sample Preparation

The investigated samples were grown using a plasma-assisted MBE (RC2100, EpiQuest, Japan) on phosphorous-doped n-type 2-inch Si(111) substrates.[36-41] A conventional solid-source effusion cell was used to supply gallium (Ga), whereas an As-valved cracker cell operated in the As_4 mode was used to supply arsenic (As). Nitrogen (N) was supplied by a radio frequency plasma source.[35] The epi-ready Si substrate facilitated NW growth development without any pretreatment because its surface was coated with a thin native oxide layer with a typical thickness of several nanometers. The presence of pinholes in the oxide layer induced the formation of nanocraters, which served as nucleation sites for the NWs.[37-40] The GaAs NW core was nucreated by the constituent Ga-induced vapor-liquid-solid growth mechanism by supplying Ga and As fluxes on the Si substrate.[37, 38, 41-45] The production of GaAs/GaInNAs (GaNAs)/GaAs core–multishell NWs is necessary to modify the flow of N atoms. The beam equivalent pressures (BEP) of As and Ga were adjusted to 6.3×10^{-4} Pa and 5.8×10^{-5} Pa, respectively, during the formation of the NW core. The As and Ga supplies corresponded to planar growth rates of 1.0 and 0.7 ML/s on a GaAs(001) substrate. These growth rates were determined by calibrating the reflection of high-energy electron diffraction oscillation.[46, 47] The V/III atomic ratio was estimated to be approximately 1.4 from the stoichiometric conditions identified by the surface reconstruction transition between As-rich (2×4) and Ga-rich (4×2) regions on the GaAs growth plane on GaAs (001).[48]

Figure 1 shows a schematic illustration of the procedure for the formation of GaAs/GaInNAs/GaAs core–multishell NWs on a 2-inch Si wafer. The growth of the GaAs core was initiated by opening the Ga shutter under As overpressure, which was grown at 560°C for 30 min. The occurrence of a growth interruption for 15 min facilitated the crystallization of the Ga catalyst and subsequently stimulated the formation of core–shell NWs through dominant lateral growth. During this interruption, the As and Ga fluxes on GaAs(001) were adjusted to 2.0 and 0.3 ML/s, respectively, to establish an adequate growth rate for the following shell layers.[37, 39] The BEP and flux of indium (In) were set to be 1.0×10^{-5} Pa and 0.1 ML/s, respectively. The concentration group-III constituents in the GaInNAs layer were designed to be 70% Ga and 30% In based on the flux ratio. The initial GaAs shell

was grown at 450°C for 7 min, whereas the N plasma was ignited. Afterward, the triple quantum-well structure of GaInNAs/GaAs was created by growing each layer for 4.5/7 min, and the sequence was repeated three times.[35] Finally, the outermost GaAs shell was grown for 20 min to form a GaAs/GaInNAs/GaAs core–multishell structure. A series of sample structures were fabricated by varying the flux of N, which was controlled by adjusting the microwave power of the plasma from 0 to 120 W at a constant N_2 gas flow rate of 0.05 sccm.[37] Based on our previous study,[49] the thickness of the GaInNAs well and GaAs barriers should be 9 nm and 11 nm, respectively. At this quantum-well width, the optical transition energy shift induced by quantum confinement would be negligible.[35] The pure Si substrate and GaAs/AlGaAs core–shell NW sample on Si(111) were prepared for comparison to facilitate the absorption measurement.[24] The composition of In and N in GaInNAs was determined from the band gaps[50] obtained from the absorption spectra, assuming the effects of quantum confinement are negligible, as will be shown in Section 3.5.

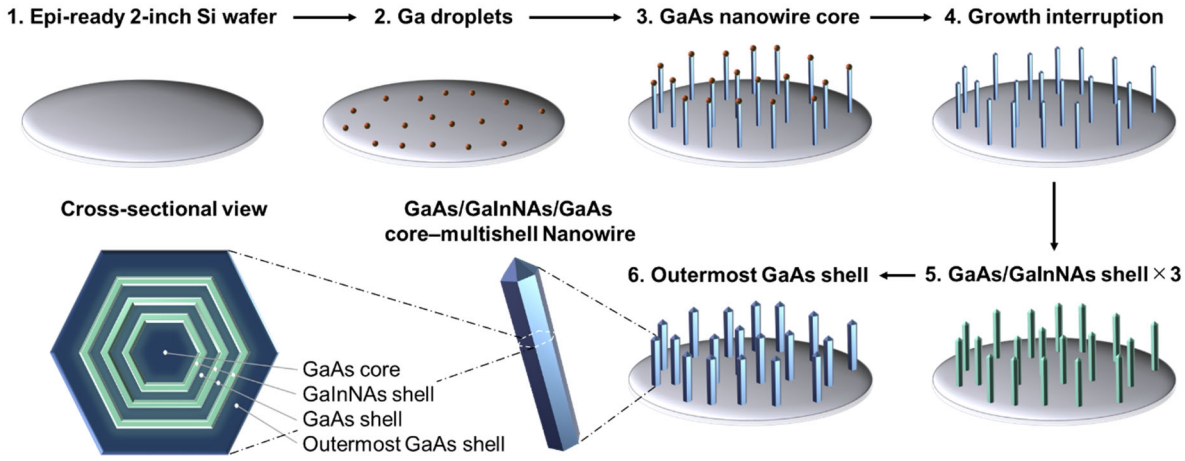


Figure 1. Schematic illustration of the procedure for the formation of GaAs/GaInNAs/GaAs core–multishell NWs on a 2-inch Si wafer.

2.2. Characterization Methods

The morphology of the NWs was analyzed using a scanning electron microscope (SEM) equipped with a JCM-7000 instrument (JEOL, Japan). The XRD measurements were conducted using the Malvern Panalytical X'Pert MRD system equipped with a graded parabolic X-ray mirror with a four-bounce Ge(220) monochromator and Cu $K\alpha_1$ radiation. A three-bounce Ge(220) analyzer and a Xe proportional detector were used to execute symmetric θ–2θ scans around the Si(111) reflection. PL measurements were conducted using a micro-PL system at RT. A 532-nm solid-state laser was used for PL excitation. The PL signal was collected in a backscattered geometry from the sample through a 20× objective

(NA = 0.5) and detected using a thermoelectrically cooled Andor iDus InGaAs array attached to a grating monochromator.

PL mapping was performed on the sample wafer using a scanning microscope equipped with a Horiba Jobin-Yvon LabRAM-HR system and an *XY*-stage. The beam spot size had a diameter of approximately 30 μm, and the scan range covered an area of 51 mm × 50 mm with a step size of 1 mm. The measurement was conducted using a neodymium-doped yttrium aluminum garnet (Nd-YAG) laser with an excitation power of 5 mW to induce 532-nm excitation at RT. The PL signal was collected using a 10× objective (NA = 0.3) with a backscattering configuration and detected using a liquid-nitrogen-cooled InGaAs detector. The spot diameter was approximated to be 30 μm based on a laser diameter of 0.7 mm and focal length of 11 mm, taking into account the empirical measurement system deviations such as optical axis misalignment and surface irregularities.[51] The wavelength variation in PL spectrum intensity by the system is calibrated using a standard white light source. The reflectance spectra of the NWs were acquired across the visible-to-NIR range using a Shimadzu (U-4100, SolidSpec-3700DUV) spectrophotometer equipped with an integrating sphere. A halogen lamp was used as the light source, and the reflected light was collected using a photomultiplier tube for wavelengths below 870 nm and an InGaAs photodetector for longer wavelengths. The spectra were calibrated with a white standard from Labsphere.

3. RESULTS AND DISCUSSION

3.1. SEM Observation

Multiple samples were prepared, with each sample containing different quantities of N introduced into the GaInNAs shell layer. In addition, GaNAs shell layer samples were prepared for comparison. Figure 2(a) shows the photograph of a 2-inch Si wafer after the NWs growth. Figures 2 (b) and (c) show the planar surface and 45°-tilted SEM micrographs, respectively, particularly on GaAs/GaInNAs/GaAs core–multishell NWs with GaInNAs shell containing 11% In and approximately 1.2% N. Additional images for other samples are provided in the supporting information. The dark region containing dense NWs demonstrated convincing light absorption. This remarkable feature is contrary to the visual characteristics of the original or unmodified Si wafer before growth. The dark region was observed over the entire substrate surface, except for the substrate edge, where the substrate holder interfered with the molecular beam flux during growth. This finding indicates that the NW array

structures can efficiently absorb light and minimize reflection, demonstrating their application potential as effective light-absorbing materials.

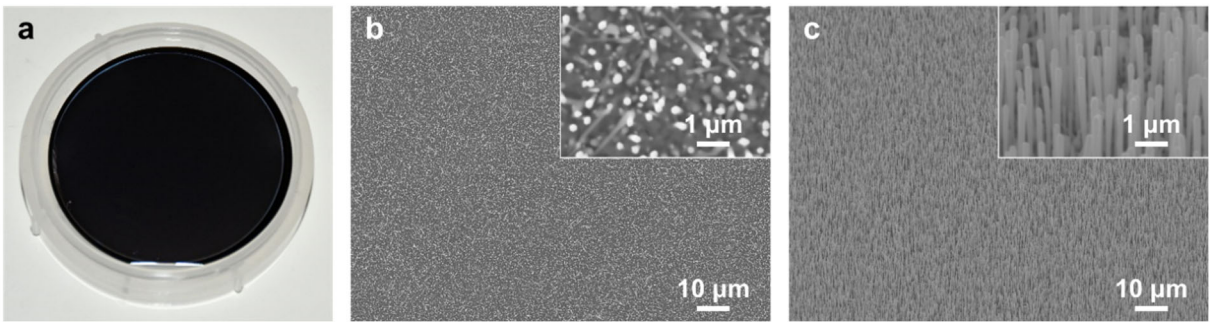


Figure 2. (a) Photograph of a 2-inch Si wafer after the growth of GaAs/GaInNAs/GaAs core–multishell NWs containing 1.2% N in the GaInNAs shell; (b) SEM image of the planar surface with an inset of higher magnification; and (c) SEM image with a 45°-tilt and an inset of higher magnification.

3.2. Distribution of NWs Length, Diameter, Density, Vertical Yield

Figure 3 presents a comprehensive overview of the NWs, including their length, diameter, NW density, and vertical yield distribution for each sample, as determined by SEM. Distinct NWs, with an average length ranging from 3.7 to 4.3 μm and average diameter between 180 and 200 nm, were observed. The presence of dense NWs on the surface exhibits an average vertical yield of 80%–90% and a density that ranges from 5.2 to 7.6 × 10^8 cm^{-2} (Fig. 3(c)), which is considered sufficiently dense in previous literature.[52] Figure 3 shows consistency in the NW arrays for all samples with regard to their length, diameter, density, and vertical yield.

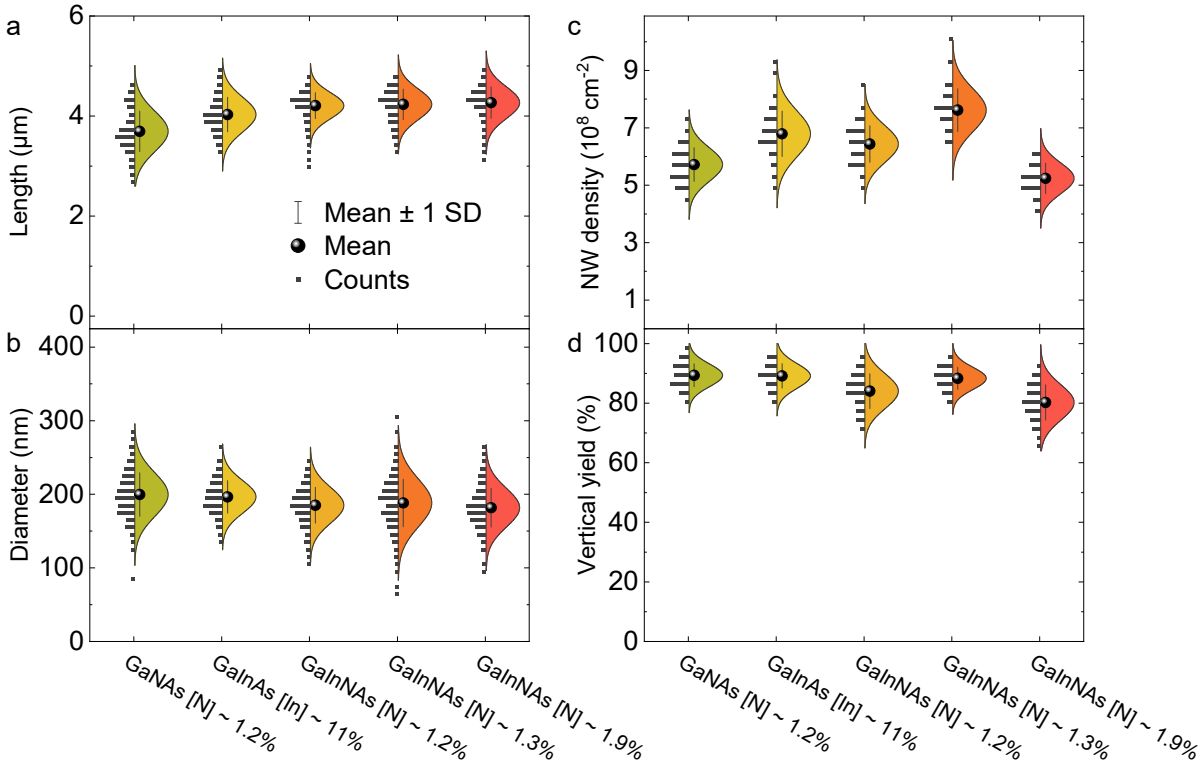


Figure 3. Violin plots showing the (a) length, (b) diameter, (c) NW density, and (d) vertical yield distribution for each NW sample, which were obtained from SEM histograms and fitted by Gaussian distributions. The error bar indicates the standard deviation.

3.3. XRD Characteristics

The results of θ–2θ XRD scans for GaAs/GaInNAs/GaAs core–multishell NWs with different quantities of In and N in the GaInNAs shell are presented in Fig. 4. The NWs in the GaInNAs shell contain 11% In and 0, 1.2%, 1.3%, or 1.9% N, whereas the GaAs/GaNAs/GaAs core–multishell NWs in the GaNAs shell contain 1.2% N.[53, 54] The centers of the curves were adjusted using the Si(111) reflection peak at 14.22° (supporting information). The peaks originating from the GaAs-related NWs were observed at 13.562° and 13.646° with regard to the Si(111) peak of the substrate. These peaks correspond to the WZ GaAs(0002) and ZB GaAs(111) planes with spacings of 0.3285 and 0.3265 nm, respectively.[55] NWs with GaInAs shells display peaks at 13.542° and 13.626°, which are larger than the lattice constant of GaAs, exhibiting a shift toward lower angles.

The GaAs(111) peak exhibited a shift toward higher angles with an increase in N content within the GaInNAs shell. This shift is attributed to the strain compensation facilitated by larger In atoms through the incorporation of smaller N atoms, which affects the entire NW structure.[50] The intensity of the WZ GaAs(0002) peak decreases as N content increases. This result is consistent with our previously reported results, that is, the ZB GaAs(111) peak in the

GaAs/GaNAs/GaAs core–multishell NWs shifts toward higher angles with the increase of N content.[34] The presence of WZ segments in NWs with GaInNAs shells can be recognized in Fig. 4. These peaks are observed at lower angles than the GaAs NWs, suggesting that they are in a compressive strain state. For NWs with GaNAs shells, the peak positions of ZB and WZ are shifted to higher angles compared to GaAs NWs, indicating that they are subjected to tensile strain.

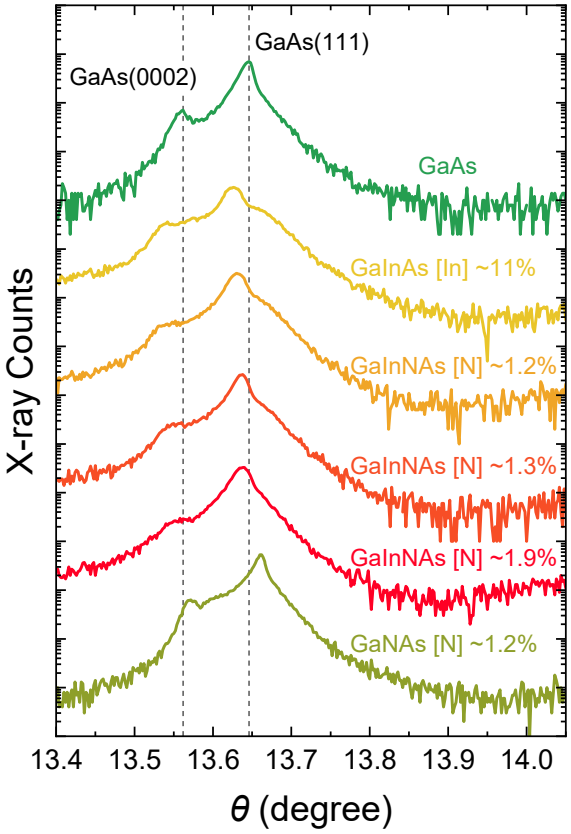


Figure 4. XRD measurements of the GaAs/GaInNAs/GaAs core–multishell NWs containing 11% In and 0, 1.2%, 1.3%, or 1.9% N in the GaInNAs shell, and the GaAs/GaNAs/GaAs core–multishell NWs containing 1.2% N in the GaNAs shell, from top to bottom.

3.4. Optical Properties

Figure 5(a) presents the results of RT micro-PL measurements on the samples. A single peak at 1051 nm is detected in the PL spectrum of NWs in a GaNAs shell containing 1.2% N. For NWs with GaInAs, a single peak at 997 nm is detected and is attributed to 11% In content. The PL peak red shifts to 1102, 1111, and 1206 nm, which is attributed to the variation in N composition.[29, 32, 50] The peaks of NWs containing 1.9% N in the GaInNAs shell evolve from NWs with the GaNAs shell to NWs with a full width at half maximum (FWHM) of 111, 154, 85, 80, and 160 meV, respectively. A summary of the correlation between the peak energy

and peak FWHM as a function of N content for the NWs with the GaInNAs shells is provided in Figs. 5(b)–(c). The GaInNAs sample with 1.2% N exhibits increased PL peak intensity and a reduced FWHM compared with GaInAs with 11% In and GaNAs with 1.2% N. This effect is attributed to the mitigation of strain deformation, facilitated by the introduction of In and N. Compared with the GaInNAs sample containing 1.2% N, the PL intensity of the sample containing 1.3% N is reduced by half. In general, the peak wavelength shifts to lower energy levels as the content of N increases (Fig. 5(b)). The GaInNAs sample containing 1.9% N shows an increase in the broadening of the PL peak widths and a decrease the PL peak intensity compared with the samples with less N. This finding could be due to the structural degradation caused by the addition of N, which include phase separation, strain accumulation, and defect formation.[32, 35, 49, 56-61] The results of the RT-PL measurements indicate that the GaInNAs sample with 11% In and 1.2% N has the highest peak intensity and narrowest FWHM. This composition is considered to be preferable for minimizing critical defect formation and achieving high crystallinity by improving alloy uniformity and strain compensation and simultaneously introducing In and N. As shown in Figs. 5 (b) and (c), this trend is reproducible and consistent for all eight GaInNAs samples.

The results of PL mapping for the GaInNAs NWs sample with 11% In and 1.2% N, which exhibiting the strongest intensity and narrowest FWHM on 2-inch Si wafer, are presented in Figs. 5(d)–(f). These figures provide information on the integrated intensity distribution, peak wavelength distribution, and FWHM distribution. As shown in Fig. 5(d), the integrated intensity was distributed with a variation of ±12.6% from the mean, and a bright and homogeneous luminescence was obtained on the entire surface of the 2-inch Si(111) substrate. The homogeneity of the PL peak wavelength distribution across the entire 2-inch Si(111) substrate is shown in Fig. 5(e), with a peak wavelength of 1099 nm and a small standard deviation of 2.7 nm. Fig. 5(f) reveals that the peak FWHM was 80 nm with a standard deviation of 3.9 nm. Therefore, the structure and composition of the GaInNAs emission layer remain homogeneous across the 2-inch Si wafer. The produced GaInNAs NWs exhibit homogeneous and luminescent characteristics, particularly in the NIR region, making them suitable for practical applications.

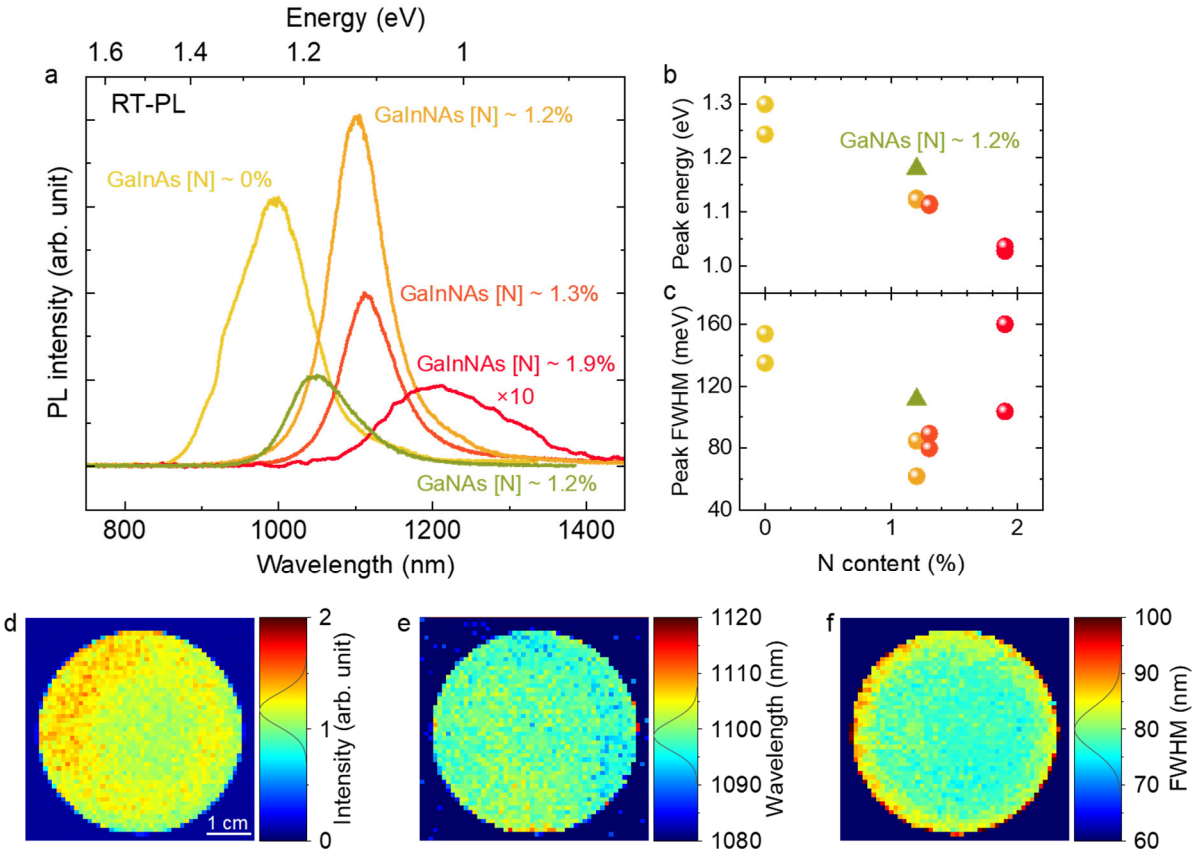


Figure 5. (a) Room-temperature photoluminescence spectra of the GaAs/GaInNAs/GaAs core–multishell NWs containing 11% In and 0, 1.2%, 1.3%, or 1.9% N in the GaInNAs shell, and the GaAs/GaNAs/GaAs core–multishell NWs containing 1.2% N in the GaNAs shell. However, in the graph of the 1.9% N sample, the vertical axis is represented by a factor of 10. (b) Peak energy and (c) peak FWHM as a function of N content for the NWs in the GaInNAs shell. A triangle symbol indicates the GaNAs sample. For reproducibility, similar samples were replicated, resulting in the duplication of data. (d)–(f) PL mapping for the GaAs/GaInNAs/GaAs core–multishell NWs containing 11%In and 1.2% N on 2-inch Si wafer with distributions of (d) intensity, (e) wavelength, and (f) FWHM. The corresponding Gaussian curves are represented on a color scale.

3.5. Reflectance Spectra

Figure 6(a) presents a collection of reflectance spectra from visible-to-NIR wavelengths for a variety of NW array samples and the pure Si substrate. The reflectance spectra for our previously reported GaAs/$Al_{0.8}Ga_{0.2}As$ core–shell NWs are also presented for comparison (Figs. 6(a)–(b)).[24] The Si substrate shows a standard pattern, with an absorption edge of approximately 1100 nm and a reflectance exceeding 50% over the spectral range. By contrast, NW samples consistently exhibit reflectance below 40% within the same spectral range; thus,

such samples drastically suppressed their reflectance compared with that of the Si substrate. NW samples show markedly low reflectance at wavelengths below the respective absorption edges, so the entire substrate was observed to be black. The results are consistent with the reflectance of vertically arrayed Si NWs and subwavelength structured surfaces on a crystalline Si substrate.[62-64] The reflectance of the GaNAs NW sample is less than 6% in the visible wavelength range of 400–800 nm, whereas the GaInAs NWs exhibit a reflectance that is less than 4%. The GaInNAs NWs exhibit low reflectance, reaching values below 2%. Figure 6(b) presents a magnified view of the reflectance spectra in the region of the absorption edge ranging from 800 to 1400 nm. The GaAs/AlGaAs NW sample displays a distinct absorption threshold at 880 nm, corresponding to the band gap of the GaAs core, whereas the GaAs/GaInNAs (GaNAs and GaInAs) NWs show a gradual absorption edge ranging from 1000 to 1200 nm.

The introduction of In and N confirms the red shift from the GaAs absorption edge of 880 nm.[31] Each absorption edge corresponds to the PL peak wavelength presented in Fig. 5(a), and the FWHM would contribute to the sharpness of the absorption edge. The GaInNAs NWs with 1.9% N shows a high PL FWHM compared with the other samples and evident changes in the reflectance spectrum, indicating the degradation of its crystal quality consistent with the PL measurements. This result is reproducible and is further elaborated in the supporting information. Besides, the PL peak intensity does not have a significant contribution to reflectance.

Tauc plots of each NWs sample are shown in Fig. 6(c), respectively. The band gap of NWs samples was estimated using Kubelka-Munk theory.[65, 66] The band gap of NWs with GaInAs is deduced to be 1.26 eV. Based on this value, the In content of the GaInAs layer is 11% if quantum confinement effects are ignored.[50] With increasing N content in the GaInNAs shell layer, the band gap shifts to 1.13, 1.12, and 1.07 eV, with corresponding N contents estimated to be 1.2, 1.3, and 1.9%, respectively. For NWs with GaNAs, the band gap is obtained to be 1.22 eV and the N content is 1.2%. These results indicate that the black color observed in the samples presented in Fig. 2(a) can be attributed to light scattering caused by the structural features of the NWs and the light absorption extending into the NIR region by the GaInNAs (GaNAs and GaInAs) shell.[67]

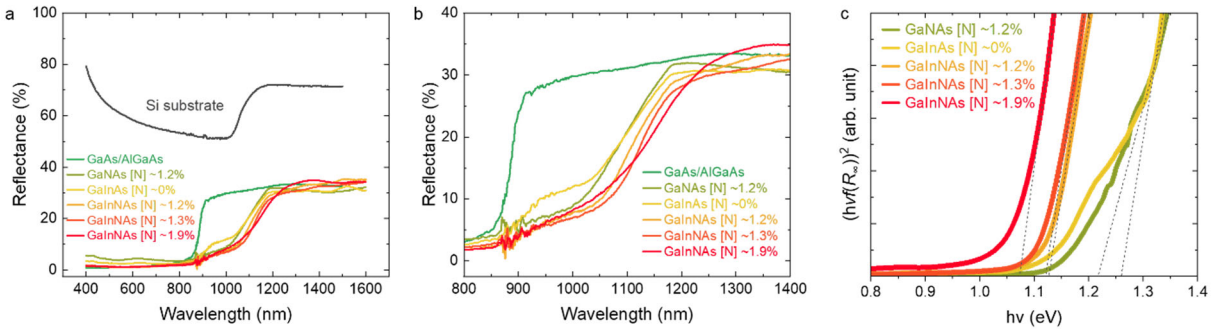


Figure 6. (a) Reflectance spectra from visible-to-NIR wavelengths for the pure Si substrate, the sample after the growth of GaAs/GaInNAs/GaAs core–multishell NWs containing 11% In and 0, 1.2%, 1.3%, or 1.9% N, and the sample after the growth of GaAs/GaNAs/GaAs core–multishell NWs containing 1.2% N. The reflectance spectra of our reported GaAs/$Al_{0.8}Ga_{0.2}As$ core–shell NW sample is included for reference.[24] Reproduced from ref 24. Available under a CC-BY 3.0 license. Copyright 2023 The Royal Society of Chemistry. (b) Magnified curve of the reflectance spectra near the absorption edge. The presence of noise in the reflectance at the approximately 870 nm visible region for all curves is ascribed to the switching of photodetectors across different response ranges. (c) Tauc plots for each NWs sample.

4. CONCLUSIONS

We have synthesized GaAs/GaInNAs/GaAs core–multishell NWs containing 11% In and 0, 1.2%, 1.3%, or 1.9% N by plasma-assisted MBE on 2-inch Si(111) substrates through Ga-induced vapor-liquid-solid growth. The fabricated samples exhibit a uniformly black color across the entire substrate, with consistent NW length and diameter. They also have a high NW density (10^8 cm^{-2} or higher) and a high vertical yield (80% or higher). XRD data show that increasing N in the GaInNAs shell causes a shift in the GaAs(111) peak position toward higher angles, which was attributed to the strain-compensating effects generated by In and N, thereby affecting the entire NW structure. An evaluation of the RT-PL reveals that the emission peaks show a red shift to approximately 1000–1200 nm as the content of N in the NWs increases. The GaInNAs sample with 11% In and 1.2% N shows homogeneous RT emission at 1100 nm across the entire surface of the 2-inch Si substrate. The reflectance of NWs is significantly reduced compared with the Si substrate across the spectral region. Remarkably, the GaInNAs NWs show low reflectance, exhibiting values less than 2% when the wavelengths are below the absorption edge. The redshift observed after the addition of In and N from the GaAs absorption edge ranging from 880 to 1000–1200 nm is consistent with

the PL results. The property exhibits application potential as a broadband NIR photoelectric conversion such as solar cells and telecommunication light sources.

SUPPORTING INFORMATION

Supporting Information for photograph and SEM observations of the samples investigated, and wide range XRD scans containing Si(111) reflection for the series of samples, and reproductivity of the reflectance measurement are available Online.

ACKNOWLEDGEMENTS

This study received partial financial support from KAKENHI (Nos. 23H00250, 21KK0068, 19H00855, and 16H05970) from the Japan Society for the Promotion of Science.

AUTHOR CONTRIBUTIONS

Keisuke Minehisa: Conceptualization (lead); Data curation (lead); Formal analysis (lead); Investigation (lead); Writing – original draft (lead).

Fumitaro Ishikawa: Conceptualization (equal); Data curation (equal); Formal analysis (equal); Funding acquisition (lead); Writing original draft (equal); Writing – review & editing (lead).

Kaito Nakama: Data curation (supporting); Investigation (supporting).

Hidetoshi Hashimoto: Data curation (supporting); Investigation (supporting).

Data availability statement

The data that support the findings of this study are available from the corresponding author upon reasonable request.

Conflict of interest disclosure

The authors declare there are no conflicting interest.

REFERENCES

[1] Tomioka, K.; Yoshimura, M.; Fukui, T. A III-V nanowire channel on silicon for high-performance vertical transistors. *Nature* **2012**, *488*, 189.

[2] Zhuang, X.; Ning, C. Z.; Pan, A. Composition and bandgap-graded semiconductor alloy nanowires. *Adv. Mater.* **2012**, *24*, 13.

[3] Yang, P.; Yan, R.; Fardy, M. Semiconductor nanowire: what's next?. *Nano Lett.* **2010**, *10*, 1529.

[4] Gudiksen, M. S.; Lauhon, L. J.; Wang, J.; Smith, D. C.; Lieber, C. M. Growth of nanowire superlattice structures for nanoscale photonics and electronics. *Nature* **2002**, *415*, 617.

[5] Garnett, E.; Mai, L.; Yang, P. Introduction: 1D Nanomaterials/Nanowires. *Chem. Rev.* **2019**, *119*, 8955.

[6] Thelander, C.; Agarwal, P.; Brongersma, S.; Eymery, J.; Feiner, L.F.; Forchel, A.; Scheffler, M.; Riess, W.; Ohlsson, B. J.; Gösele, U.; Samuelson, L. Nanowire-based one-dimensional electronics. *Mater. Today* **2006**, *9*, 28.

[7] Xia, X.; Tu, J.; Zhang, Y.; Wang, X.; Gu, C.; Zhao, X. B.; Fan, H. J. High-quality metal oxide core/shell nanowire arrays on conductive substrates for electrochemical energy storage. *ACS Nano* **2012**, *6*, 5531.

[8] Kolmakov, A.; Moskovits, M. Chemical sensing and catalysis by one-dimensional metal-oxide nanostructures. *Annu. Rev. Mater. Res.* **2004**, *34*, 151.

[9] Chen, R.; Tran, T. D.; Ng, K. W.; Ko, W. S.; Chuang, L. C.; Sedgwick, F. G.; Chang-Hasnain, C. Nanolasers grown on silicon. *Nat. Photonics* **2011**, *5*, 170.

[10] Hersee, S. D.; Sun, X.; Wang, X. The controlled growth of GaN nanowires. *Nano Lett.* **2006**, *6*, 1808.

[11] Mårtensson, T.; Svensson, C. P. T.; Wacaser, B. A.; Larsson, M. W.; Seifert, W.; Deppert, K.; Gustafsson, A.; Wallenberg, L. R.; Samuelson, L. Epitaxial III−V Nanowires on Silicon. *Nano Lett.* **2004**, *4*, 1987.

[12] Lauhon, L. J.; Gudiksen, M. S.; Wang, D.; Lieber, C. M. Epitaxial core-shell and core-multishell nanowire heterostructures. *Nature* **2002**, *420*, 57.

[13] Tomioka, K.; Tanaka, T.; Hara, S.; Hiruma, K.; Fukui, T. III–V Nanowires on Si Substrate: Selective-Area Growth and Device Applications. *IEEE J. Sel. Top. Quantum Electron.* **2011**, *17*, 1112.

[14] Xiang, J.; Lu, W.; Hu, Y.; Wu, Y.; Yan, H.; Lieber, C. M. Ge/Si nanowire heterostructures as high-performance field-effect transistors. *Nature* **2006**, *441*, 489.

[15] Li, Y.; Xiang, J.; Qian, F.; Gradecak, S.; Wu, Y.; Yan, H.; Blom, D. A.; Lieber, C. M. Dopant-free GaN/AlN/AlGaN radial nanowire heterostructures as high electron mobility transistors. *Nano Lett.* **2006**, *6*, 1468.

[16] Dillen, D. C.; Kim, K.; Liu, E. S.; Tutuc, E. Radial modulation doping in core-shell nanowires. *Nat. Nanotechnol.* **2014**, *9*, 116.

[17] Tomioka, K.; Motohisa, J.; Hara, S.; Hiruma, K.; Fukui, T. GaAs/AlGaAs core multishell nanowire-based light-emitting diodes on Si. *Nano Lett.* **2010**, *10*, 1639.

[18] Tang, J.; Huo, Z.; Brittman, S.; Gao, H.; Yang, P. Solution-processed core-shell nanowires for efficient photovoltaic cells. *Nat. Nanotechnol.* **2011**, *6*, 568.

[19] Wang, S.; Yan, X.; Zhang, X.; Li, J.; Ren, X. Axially connected nanowire core-shell pn junctions: a composite structure for high-efficiency solar cells. *Nanoscale Res. Lett.* **2015**, *10*, 1.

[20] Åberg, I.; Vescovi, G.; Asoli, D.; Naseem, U.; Gilboy, J. P.; Sundvall, C.; Dahlgren, A.; Svensson, K. E.; Anttu, N.; Björk, M. T.; Samuelson, L. A GaAs nanowire array solar cell with 15.3% efficiency at 1 sun. *IEEE J. photovoltaics* **2015**, *6*, 185.

[21] Prete, P.; Lovergine, N. Dilute nitride III-V nanowires for high-efficiency intermediate-band photovoltaic cells: Materials requirements, self-assembly methods and properties. *Prog. Cryst. Growth Charact. Mater.* **2020**, *66*, 100510.

[22] Wu, Y.; Yan, H.; Yang, P. Semiconductor nanowire array: potential substrates for photocatalysis and photovoltaics. *Top. Catal.* **2002**, *19*, 197.

[23] Jia, C.; Lin, Z.; Huang, Y.; Duan, X. Nanowire Electronics: From Nanoscale to Macroscale. *Chem. Rev.* **2019**, *119*, 9074.

[24] Minehisa, K.; Murakami, R.; Hashimoto, H.; Nakama, K.; Sakaguchi, K.; Tsutsumi, R.; Tanigawa, T.; Yukimune, M.; Nagashima, K.; Yanagida, T.; Sato, S.; Hiura, S.; Murayama, A.; Ishikawa, F. Wafer-scale integration of GaAs/AlGaAs core-shell nanowires on silicon by the single process of self-catalyzed molecular beam epitaxy. *Nanoscale Adv.* **2023**, *5*, 1651.

[25] Amemiya, K.; Shimizu, Y.; Koshikawa, H.; Shitomi, H.; Yamaki, T. Supreme-black levels enabled by touchproof microcavity surface texture on anti-backscatter matrix. *Sci. Adv.* **2023**, *9*, eade4853.

[26] Krogstrup, P.; Jørgensen, H. I.; Heiss, M.; Demichel, O.; Holm, J. V.; Aagesen, M.; Nygard, J.; Fontcuberta i Morral, A. Single-nanowire solar cells beyond the Shockley–Queisser limit. *Nat. photonics* **2013**, *7*, 306.

[27] Cretì, A.; Prete, P.; Lovergine, N.; Lomascolo, M. Enhanced optical absorption of GaAs near-band-edge transitions in GaAs/AlGaAs core–shell nanowires: implications for nanowire solar cells. *ACS Appl. Nano Mater.* **2022**, *5*, 18149.

[28] Kondow, M.; Uomi, K.; Hosomi, K.; Mozume, T. Gas-source molecular beam epitaxy of GaNxAs1-x using a N radical as the N source. *Jpn J. Appl. Phys.* **1994**, *33*, L1056.

[29] Shan, W.; Walukiewicz, W.; Ager, J. W.; Haller, E. E.; Geisz, J. F.; Friedman, D. J.; Olson, J. M.; Kurtz, S. R. Band anticrossing in GaInNAs alloys. *Phys. Rev. Lett.* **1999**, *82*, 1221.

[30] Henini, M. *Dilute Nitride Semiconductors*, Elsevier, New York, **2004**.

[31] Weyers, M.; Sato, M.; Ando, H. Red shift of photoluminescence and absorption in dilute GaAsN alloy layers. *Jpn. J. Appl. Phys.* **1992**, *31*, L853.

[32] Yukimune, M.; Fujiwara, R.; Ikeda, H.; Yano, K.; Takada, K.; Jansson, M.; Chen, W. M.; Buyanova, I. A.; Ishikawa, F. GaAs/GaNAs core-multishell nanowires with nitrogen composition exceeding 2%. *Appl. Phys. Lett.* **2018**, *113*, 011901.

[33] Chen, S.; Yukimune, M.; Fujiwara, R.; Ishikawa, F.; Chen, W. M.; Buyanova, I. A. Near-infrared lasing at 1 μm from a dilute-nitride-based multishell nanowire. *Nano Lett.* **2019**, *19*, 885.

[34] Yukimune, M.; Fujiwara, R.; Mita, T.; Ishikawa, F. Polytypism in GaAs/GaNAs core-shell nanowires. *Nanotechnol.* **2020**, *31*, 505608.

[35] Nakama, K.; Yukimune, M.; Kawasaki, N.; Higo, A.; Hiura, S.; Murayama, A.; Jansson, M.; Chen, W. M.; Buyanova, I. A.; Ishikawa, F. GaAs/GaInNAs core-multishell nanowires with a triple quantum-well structure emitting in the telecommunication range. *Appl. Phys. Lett.* **2023**, *123*, 081104.

[36] Colombo, C.; Spirkoska, D.; Frimmer, M.; Abstreiter, G.; Fontcuberta i Morral, A. Ga-assisted catalyst-free growth mechanism of GaAs nanowires by molecular beam epitaxy. *Phys. Rev. B* **2008**, *77*, 155326.

[37] Ahn, N.; Araki, Y.; Kondow, M.; Yamaguchi, M.; Ishikawa, F. Effects of growth interruption, As and Ga fluxes, and nitrogen plasma irradiation on the molecular beam epitaxial growth of GaAs/GaAsN core–shell nanowires on Si (111). *Jpn. J. Appl. Phys.* **2014**, *53*, 065001.

[38] Fontcuberta i Morral, A.; Colombo, C.; Abstreiter, G.; Arbiol, J.; Morante, J. R. Nucleation mechanism of gallium-assisted molecular beam epitaxy growth of gallium arsenide nanowires. *Appl. Phys. Lett.* **2008**, *92*, 063112.

[39] Paek, J. H.; Nishiwaki, T.; Yamaguchi, M.; Sawaki, N. Catalyst free MBE-VLS growth of GaAs nanowires on (111)Si substrate. *Phys. Status Solidi (C)* **2009**, *6*, 1436.

[40] Paek, J.; Yamaguchi, M.; Amano, H. MBE–VLS growth of catalyst-free III–V axial heterostructure nanowires on (1 1 1) Si substrates. *J. Cryst. Growth* **2011**, *323*, 315.

[41] Araki, Y.; Yamaguchi, M.; Ishikawa, F. Growth of dilute nitride GaAsN/GaAs heterostructure nanowires on Si substrates. *Nanotechnol.* **2013**, *24*, 065601.

[42] Mandl, B.; Stangl, J.; Hilner, E.; Zakharov, A. A.; Hillerich, K.; Dey, A. W.; Samuelson, L.; Bauer, G.; Deppert, K.; Mikkelsen, A. Growth mechanism of self-catalyzed group III− V nanowires. *Nano Lett.* **2010**, *10*, 4443.

[43] Wagner, R. S.; Ellis, W. C. Vapor-liquid-solid mechanism of single crystal growth. *Appl. Phys. Lett.* **1964**, *4*, 89.

[44] Harmand, J. C.; Tchernycheva, M.; Patriarche, G.; Travers, L.; Glas, F.; Cirlin, G. GaAs nanowires formed by Au-assisted molecular beam epitaxy: Effect of growth temperature. *J. Cryst. Growth* **2007**, *301-302*, 853.

[45] Perea, D. E.; Allen, J. E.; May, S. J.; Wessels, B. W.; Seidman, D. N.; Lauhon, L. J. Three-dimensional nanoscale composition mapping of semiconductor nanowires. *Nano Lett.* **2006**, *6*, 181.

[46] Zhang, J.; Neave, J. H.; Dobson, P. J.; Joyce, B. A. Effects of diffraction conditions and processes on rheed intensity oscillations during the MBE growth of GaAs. *Appl. Phys. A* **1987**, *42*, 317.

[47] Ishikawa, F.; Trampert, A.; Ploog, K. H. Low substrate temperature and low As-pressure growth concept for the molecular beam epitaxial growth of 1.55 μm (Ga, In)(N, As) multiple quantum wells. *J. Cryst. Growth* **2007**, *301-302*, 529.

[48] Däweritz, L.; Hey, R. Reconstruction and defect structure of vicinal GaAs (001) and $Al_xGa_{1-x}As$ (001) surfaces during MBE growth. *Surf. Sci.* **1990**, *236*, 15.

[49] Yukimune, M.; Fujiwara, R.; Mita, T.; Tsuda, N.; Natsui, J.; Shimizu, Y.; Jansson, M.; Balagula, R.; Chen, W. M.; Buyanova, I. A.; Ishikawa, F. Molecular beam epitaxial growth of dilute nitride GaNAs and GaInNAs nanowires. *Nanotechnol.* **2019**, *30*, 244002.

[50] Vurgaftman, I.; Meyer, J. R. Band parameters for nitrogen-containing semiconductors. *J. Appl. Phys.* **2003**, *94*, 3675.

[51] Saleh, B. E. A.; Teich, M. C. *Fundamentals of Photonics (2nd ed.)*, Wiley-Interscience, **2007**.

[52] Somaschini, C.; Bietti, S.; Trampert, A.; Jahn, U.; Hauswald, C.; Riechert, H.; Sanguinetti, S.; Geelhaar, L. Control over the number density and diameter of GaAs nanowires on Si (111) mediated by droplet epitaxy. *Nano Lett.* **2013**, *13*, 3607.

[53] Wu, S.; Kato, M.; Uchiyama, M.; Higashi, K.; Ishikawa, F.; Kondow, M. Nitrogen gas flow driven unintentional incorporation of Al during the growth of dilute nitride

semiconductor by plasma-assisted molecular beam epitaxy. *Appl. Phys. Express* **2008**, *1*, 035004.

[54] Ishikawa, F.; Wu, S.; Kato, M.; Uchiyama, M.; Higashi, K.; Kondow, M. Unintentional source incorporation in plasma-assisted molecular beam epitaxy. *Jpn. J. Appl. Phys.* **2009**, *48*, 125501.

[55] Jahn, U.; Lähnemann, J.; Pfüller, C.; Brandt, O.; Breuer, S.; Jenichen, B.; Ramsteiner, M.; Geelhaar, L.; Riechert, H. Luminescence of GaAs nanowires consisting of wurtzite and zinc-blende segments. *Phys. Rev. B* **2012**, *85*, 045323.

[56] Mussler, G.; Chauveau, J. M.; Trampert, A.; Ramsteiner, M.; Däweritz, L.; Ploog, K. H. Nitrogen-dependent optimum annealing temperature of Ga (As, N). *J. Cryst. Growth* **2004**, *267*, 60.

[57] Toivonen, J.; Tuomi, T.; Riikonen, J.; Knuuttila, L.; Hakkarainen, T.; Sopanen, M.; Lipsanen, H.; McNally, P. J.; Chen, W.; Lowney, D. Misfit dislocations in GaAsN/GaAs interface. *Sci. Mater. Electron.* **2003**, *14*, 267.

[58] Buyanova, I. A.; Chen, W. M.; Tu, C. W. Defects in dilute nitrides. *J. Phys.: Condens. Matter* **2004**, *16*, S3027.

[59] Filippov, S.; Ishikawa, F.; Chen, W. M.; Buyanova, I. A. Structural properties of GaNAs nanowires probed by micro-Raman spectroscopy. *Semicond. Sci. Technol.* **2016**, *31*, 025002.

[60] Chen, S. L.; Chen, W. M.; Ishikawa, F.; Buyanova, I. A. Suppression of non-radiative surface recombination by N incorporation in GaAs/GaNAs core/shell nanowires. *Sci. Rep.* **2015**, *5*, 11653.

[61] Buyanova, I. A.; Chen, W. M. Dilute nitrides-based nanowires—a promising platform for nanoscale photonics and energy technology. *Nanotechnol.* **2019**, *30*, 292002.

[62] Wang, X.; Pey, K. L.; Yip, C. H.; Fitzgerald, E. A.; Antoniadis, D. A. Vertically arrayed Si nanowire/nanorod-based core-shell pn junction solar cells. *J. Appl. Phys.* **2010**, *108*, 124303.

[63] Peng, K.; Wu, Y.; Fang, H.; Zhong, X.; Xu, Y.; Zhu, J. Uniform, axial-orientation alignment of one-dimensional single-crystal silicon nanostructure arrays. *Angew. Chem. Int. Ed. Engl.* **2005**, *44*, 2737.

[64] Kanamori, Y.; Sasaki, M.; Hane, K. Broadband antireflection gratings fabricated upon silicon substrates. *Opt. Lett.* **1999**, *24*, 1422.

[65] Yang, L.; Kruse, B. Revised kubelka–munk theory. i. theory and application. *J. Opt. Soc. Am. A* **2004**, *21*, 1933.

[66] Sarkar, K.; Palit, M.; Banerji, P.; Chattopadhyay, S.; Halder, N. N.; Biswas, P.; Nagabhusan, B.; Chowdhury, S. Silver catalyzed growth of $In_xGa_{1-x}As$ nanowires on Si(001) by metal–organic chemical vapor deposition. *Cryst. Eng. Comm.* **2015**, *17*, 8519.
[67] Yang, C. S.; Chang, C. H.; Lin, M. H.; Yu, P.; Wada, O.; Pan, C. L. THz conductivities of indium-tin-oxide nanowhiskers as a graded-refractive-index structure. *Opt. Express* **2012**, *20*, A441.

Table of contents

Homogeneous Large-Scale Synthesis of GaAs/GaInNAs/GaAs Nanowires on a Si Wafer for Devices Operating in the Near-Infrared Region

Keisuke Minehisa, Kaito Nakama, Hidetoshi Hashimoto, Fumitaro Ishikawa**

Research Center for Integrated Quantum Electronics, Hokkaido University, North 13 West 8, Sapporo, 060-0813, Japan

*Corresponding authors

E-mail: minehisa.keisuke@rciqe.hokudai.ac.jp (K. M.),

ishikawa.fumitaro@rciqe.hokudai.ac.jp (F. I.)

